PLOS COMPUTATIONAL BIOLOGY

RESEARCH ARTICLE

Modeling influenza seasonality in the tropics and subtropics

Haokun Yuan[1☯], **Sarah C. Kramer**[2☯¤], **Eric H. Y. Lau**[3,4], **Benjamin J. Cowling**[3,4], **Wan Yang**[1*]

1 Department of Epidemiology, Mailman School of Public Health, Columbia University, New York, New York, United States of America, **2** Department of Environmental Health Sciences, Mailman School of Public Health, Columbia University, New York, New York, United States of America, **3** World Health Organization Collaborating Centre for Infectious Disease Epidemiology and Control, School of Public Health, Li Ka Shing Faculty of Medicine, the University of Hong Kong, Hong Kong Special Administrative Region, People's Republic of China, **4** Laboratory of Data Discovery for Health Limited, Hong Kong Science Park, New Territories, Hong Kong Special Administrative Region, People's Republic of China

☯ These authors contributed equally to this work.
¤ Current address: Infectious Disease Epidemiology group, Max Planck Institute for Infection Biology, Campus Charité Mitte, Charité–Universitätsmedizin Berlin, Berlin, Germany
* wy2202@columbia.edu

Citation: Yuan H, Kramer SC, Lau EHY, Cowling BJ, Yang W (2021) Modeling influenza seasonality in the tropics and subtropics. PLoS Comput Biol 17(6): e1009050. https://doi.org/10.1371/journal.pcbi.1009050

Editor: Ruy M. Ribeiro, Los Alamos National Laboratory, UNITED STATES

Received: October 14, 2020

Accepted: May 7, 2021

Published: June 9, 2021

Data Availability Statement: We do not have permission to publish the influenza surveillance data used in this study. However, data from 2014 onwards are publicly available from https://www.chp.gov.hk/en/statistics/data/10/641/642/2274.html. For full access of the data, please contact crystal_hk_lai@dh.gov.hk at Hong Kong Center for Health Protection. Climate data are publicly available from https://www.hko.gov.hk/tc/cis/climat.htm and compiled daily temperature and specific humidity data used in this study are available at https://github.com/wan-yang/flu-subtropic-climate-models.

Abstract

Climate drivers such as humidity and temperature may play a key role in influenza seasonal transmission dynamics. Such a relationship has been well defined for temperate regions. However, to date no models capable of capturing the diverse seasonal pattern in tropical and subtropical climates exist. In addition, multiple influenza viruses could cocirculate and shape epidemic dynamics. Here we construct seven mechanistic epidemic models to test the effect of two major climate drivers (humidity and temperature) and multi-strain co-circulation on influenza transmission in Hong Kong, an influenza epidemic center located in the subtropics. Based on model fit to long-term influenza surveillance data from 1998 to 2018, we found that a simple model incorporating the effect of both humidity and temperature best recreated the influenza epidemic patterns observed in Hong Kong. The model quantifies a bimodal effect of absolute humidity on influenza transmission where both low and very high humidity levels facilitate transmission quadratically; the model also quantifies the monotonic but nonlinear relationship with temperature. In addition, model results suggest that, at the population level, a shorter immunity period can approximate the co-circulation of influenza virus (sub)types. The basic reproductive number R_0 estimated by the best-fit model is also consistent with laboratory influenza survival and transmission studies under various combinations of humidity and temperature levels. Overall, our study has developed a simple mechanistic model capable of quantifying the impact of climate drivers on influenza transmission in (sub)tropical regions. This model can be applied to improve influenza forecasting in the (sub)tropics in the future.

Funding: HY and WY were supported by the NIH (AI135926 and ES009089). SCK was supported by the NIH (T32ES023770 and F31AI138410). EHYL and BJC were supported by the Theme-based Research Scheme project no. T11-712/19-N, the University Grants Committee of the Hong Kong Government. The funders had no role in study design, data collection and analysis, decision to publish, or preparation of the manuscript.

Competing interests: I have read the journal's policy and the authors of this manuscript have the following competing interests: BJC reports receipt of honoraria from Roche and Sanofi. The rest of the authors have declared that no competing interests exist.

Author summary

Humidity has been shown to affect winter-time influenza epidemics in temperate regions. However, humidity alone is insufficient to explain the bi-annual epidemics observed in tropics and subtropics. Here we construct seven mechanistic models and test the impact of climate drivers under different hypotheses. Using surveillance data collected in Hong Kong, we identify a best-fit model capable of recreating the long-term influenza transmission dynamics observed over 20 years. The best-fit model quantifies how temperature moderates the bimodal effect of humidity on influenza transmission. The best-fit model also generates estimates of the basic reproductive number R_0 consistent with laboratory influenza survival and transmission studies under various combinations of humidity and temperature levels. Our model is fairly simple and can be easily incorporated with epidemic models (e.g., the Susceptible-Infectious-Recovered-Susceptible model) to improve influenza forecasting performance for tropical and subtropical regions.

Introduction

Influenza is a disease of considerable public health concern, causing roughly 300,000–650,000 deaths and 3–5 million cases of severe illness each year worldwide [1]. Although evidence suggests that the burden of influenza in the tropics and subtropics is not substantially less than in temperate regions [2,3], studies on influenza in these regions are comparatively rare. Likewise, modeling and forecasting efforts, which may promote both understanding of and preparation for outbreaks in the future, have mostly been focused on countries with temperate climates [4,5]. A variety of factors contribute to this disparity, including lack of long-term surveillance data and competing public health interests [6–8]. We focus here on two features of influenza epidemics in these regions that particularly complicate modeling efforts, i.e., the lack of understanding of climatic drivers and cocirculation of multiple influenza types and subtypes.

In temperate regions, influenza displays a clear seasonal pattern, with epidemics occurring in the winter and very few cases observed during the summer [9,10]. While several potential drivers of this pattern have been suggested [9], humidity appears to be particularly important in driving these "seasonal" influenza epidemics. Specifically, both survival and transmission of the influenza virus are heightened when absolute humidity (AH) is low [11], corresponding to the yearly observed peaks of influenza activity in winter [12].

In tropical or subtropical locations, this seasonal pattern is less commonly observed. Instead, influenza causes multiple epidemics each year, or else is present year-round with unpredictable variation in intensity [3,9,10,13]. In addition, humidity is relatively high all year in the tropics and subtropics, and influenza epidemics tend to occur during the rainy season, when humidity is particularly high [13,14]. Thus, the relationship observed in temperate regions and modeled by Shaman et al. [12], where influenza transmission decreases monotonically with increasing AH, is not sufficient to explain patterns in influenza transmission in the tropics and subtropics [9,15].

While the exact impacts remain unclear, humidity, precipitation and temperature are the main contenders as climate drivers for influenza transmission in the tropics and subtropics. A few studies suggest that the impact of humidity on influenza transmission may be bimodal, rather than unimodally decreasing as suggested by Shaman at al. [11,12]. Work by Yang et al. showed that influenza virus survival is higher at lower relative humidity (<50%), but also found increased survival at very high levels of relative humidity (~100%) [16]. By analyzing patterns of influenza transmission in 78 locations worldwide, Tamerius et al. [14] found that

influenza outbreaks in locations that experience high temperature and high AH year-round had a tendency to occur during the rainy season, when both AH and rainfall were high. This pattern has been consistently reported in several countries [6,17–19]. Deyle et al. [20] instead suggested that influenza transmission is driven by AH, moderated by temperature. Specifically, they find that influenza activity decreases with increasing AH up to about 24˚C (75˚F), then increases with increasing AH up to about 30˚C (86˚F), at which point high temperatures strongly restrict influenza transmission.

In addition to diverse climate drivers, co-circulation of multiple influenza viruses may contribute to the observed multiple yearly influenza epidemics in the tropics and subtropics. Circulating human influenza viruses are classified into types (A or B, based on genus) and, among influenza A viruses, subtypes (based on the genetic sequences of the hemagglutinin and neuraminidase surface proteins) [21]. Currently, circulating human influenza viruses consist of the A(H1N1) and A(H3N2) influenza subtypes, as well as influenza B viruses [1]. While influenza viruses evolve quickly, significant antigenic change only occurs over a period of one to ten years [22,23]. However, while the extent of cross-immunity between influenza (sub)types remains unknown, current influenza vaccines are not sufficient to protect people from all (sub)types of influenza virus [21,24]. Thus, we may expect that separate epidemics within a single year are often caused by different influenza viruses. As a result, appropriate models of influenza transmission in tropical and subtropical locations may need to take multiple types and subtypes into account, further complicating modeling efforts.

Here, we utilize influenza incidence data that have been collected since 1998 in Hong Kong, a densely populated city with a subtropical climate, to explore the impact of climate drivers on influenza epidemics. We formulate seven models, each allowing for differing roles of humidity, temperature, and influenza co-circulation. We expect that, by accounting for 1) increased transmission at both low and high values of AH, 2) decreased transmission at high temperatures (e.g., >30˚C), and 3) co-circulation of several influenza types and subtypes, the model best representing the impact of key climate drivers and influenza co-circulation will be able to best reproduce observed influenza dynamics in Hong Kong. In addition, influenza pandemics could occur "off-season" under more extreme climate conditions (e.g., hot summer days), due to higher population susceptibility to a novel virus. Thus, we include the 2009 pandemic in our model testing and expect the best-performing model to also capture influenza dynamics during the pandemic after accounting for the increased population susceptibility. To model the impact of humidity, here we focus on AH as it is independent of temperature. Specifically, unlike relative humidity measuring the amount of water vapor (i.e., moisture) in the air relative to the total amount of vapor that can exist in the air at its current temperature, AH measures the actual amount of water vapor in the air irrespective of the air's temperature.

Methods

Influenza data

Data on influenza-like illness (ILI) and laboratory-confirmed influenza from January 1998 through December 2018 were obtained from the Centre for Health Protection of the Hong Kong Special Administrative Region. ILI data were collected by a sentinel surveillance network consisting of 64 public out-patient clinics and roughly 50 private medical practitioners' clinics throughout Hong Kong, while laboratory testing was performed on specimens from outpatient clinics and public hospitals. Throughout our study period (21 years from January 1998 to December 2018), the same procedure for selecting specimens for viral testing was used; however, from February 10, 2014 onward, viral testing was carried out using molecular testing instead of viral culture. We multiply weekly ILI case counts by the proportion of tests positive

for influenza each week and refer to the resulting, more specific measure as ILI+. Finally, data were converted to rates per 100,000 population.

Climate data

Hong Kong has a humid subtropical climate, with hot, humid, and rainy summers, and mild winters [25]. Daily mean temperature and relative humidity were taken at the Hong Kong Observatory [26]. Using these data, we used the Clausius-Clapeyron relation [27] to calculate daily mean specific humidity, a measure of AH (see Supplementary Materials).

Model hypotheses

In this work, we formulated seven models to test several hypotheses concerning the impact of humidity and temperature on influenza transmission in Hong Kong, and how co-circulation influenza (sub)types affect this process. While specific methodology associated with each model is detailed below, we describe the hypotheses considered here:

- Null hypothesis 1 (or Null1, Constant basic reproductive number R_0): Climate conditions have no effect on influenza transmission. To represent this, we held R_0, the epidemic parameter representing the average number of new cases arising from a primary case in a fully susceptible population, constant.
- Null hypothesis 2 (or Null2, Temperate Forcing): AH affects influenza transmission in the subtropics and tropics in the same manner as in temperate regions; that is, R_0 increases monotonically with decreasing AH. Here, R_0 was modeled according to the equation first presented in [11]. This model has previously been shown to perform well when modeling influenza transmission patterns in temperate regions [12].
- AH model: The effect of AH is bimodal, with both low and high AH conditions favoring influenza transmission. Temperature is assumed to have no additional effect on transmission. R_0 was modeled according to Eq S6, where both low and high values of AH lead to higher values of R_0.
- AH/T model: Absolute humidity has a bimodal effect on R_0, as in the AH model, but this effect is moderated by temperature as shown in Eq 3. Briefly, low temperatures promote influenza transmission, and temperatures above a certain threshold limit transmission.
- AH/T/Strain: AH and temperature impact R_0 as in the AH/T model. Additionally, two "strains" of influenza co-circulate in the population, as in [12]. Here we ignore cross-immunity between strains; in other words, infection with one strain has no effect on the potential for later infection with the other strain.
- AH/T/Short: Climate forcing is included as in the AH/T model. Additionally, we restrict the duration of immunity in the model to be about 1 year (i.e., 0.5–1.5 years), in order to implicitly take co-circulation into account (i.e., for an individual, multiple infections by different influenza strains could occur within a short time span).
- AH/T/Vary: Climate forcing is included as in the AH/T model. Additionally, a small proportion (<50%) of the population experiences a significantly truncated duration of immunity (<1 year) after infection. In other words, duration of immunity to influenza is heterogeneous among the population.

SIRS model

We modeled influenza transmission in Hong Kong using a compartmental susceptible-infected-recovered-susceptible (SIRS) model with demography. While we used two distinct forms of the model for this project described below, the basic model takes the form:

$$\begin{cases} \frac{dS}{dt} = \frac{N-S-I}{L} - \frac{\beta_t I^p S}{N} - \alpha + \mu(N-S) \\ \frac{dI}{dt} = \frac{\beta_t I^p S}{N} - \frac{I}{D} + \alpha - \mu I \end{cases} \quad (1)$$

where N is the size of the model population (here set to 100,000); β_t represents the rate of transmission on day t, depending on climatic functions as described below; D is the mean infectious period; L is the average duration of immunity; and α represents random seeding from outside the model population (here we arbitrarily set it to 0.1, i.e., 1 per 10 days for all models. However, sensitivity analysis using values ranging from 1/30 to 1 showed similar results; see S1 Text). μ is the rate of natural birth and death (i.e., to maintain a constant population size, we assume equal birth and death rates). We set μ to be 0.00918 divided by 365, or the average daily birth rate per person in Hong Kong during 1998–2017 [28]. The parameter p is an exponent to introduce nonlinearity into the infection process (i.e., imperfect population mixing). The inclusion of this parameter has been shown to be helpful in modeling complicated epidemics using very simple models [29], as is the case in this work. Finally, because the 2009 pandemic was caused by a novel strain of influenza with little prior population immunity, we reset the number of susceptibles in our population in early August of 2009 to be between 60% and 80% of the total population [30–32] (vs. 40–80% for model initiation in January 1998; see Table 1). All models were run stochastically, as described in the S1 Text and in [12].

SIRS model variations

In this work, we considered three models to account for cocirculation and heterogenous immunity period:

1. **AH/T/Strain:** To account for co-circulating influenza viruses, we ran two SIRS simulations (Eq 1) in parallel, as done in Shaman et al. [12]. While there are three co-circulating influenza (sub)types, we combined A(H1N1) and B for simplicity, given the similar timing of the circulation of these two viruses (S1 Fig). Here, we applied random seeding at each week only to the "strain" that had the greater number of positive tests that week. If both "strains" were equally common, seeding was applied to a single strain at random. We then combined the output of the two simulations and compared the resulting estimates to the overall ILI+ data. Note that per this simple model, multiple influenza epidemics due to different influenza viruses can occur at the same time, as well as co-infection of multiple influenza viruses.
2. **AH/T/Short:** This model used Eq 1 but restricted L, the duration of immunity, to be between around one year to account for multiple infections within a year due to multiple circulating strains.
3. **AH/T/Vary:** In this model, a small proportion of the population loses immunity to influenza at an accelerated rate. This was modeled by replacing the term $\frac{N-S-I}{L}$ in Eq 1 with:

$$\rho \frac{\beta_{t-L_s} I^p_{t-L_s} S_{t-L_s}}{N} + (1-\rho)\frac{N-S-I}{L} \quad (2)$$

Table 1. Descriptions and estimates of the parameter ranges. The estimated parameter ranges are the 95% highest density intervals, obtained after two rounds of parameter selection from the initial ranges (shown in parentheses).

Parameter and sources of initial ranges	Parameter Description	Null1	Null2	AH	AH/T	AH/T/ Strain	AH/T/ Short	AH/T/ Vary
R_0 [12,34,36–38]	The basic reproductive number (i.e., the average number of cases caused by a primary case in a fully susceptible population)	2.06–2.11 (1.0–3.0)	NA	NA	NA	NA	NA	NA
R_{0max} [12,34,36–38]	The theoretical value of R_0 at $q = q_{min}$ and $q = q_{max}$, when $T = T_c$	NA	2.52–2.69 (1.5–3.0)	1.95–2.50 (1.5–3.0)	2.34–2.93 (1.5–3.0)	2.38–2.88 (1.5–3.0)	2.13–2.67 (1.5–3.0)	2.27–2.66 (1.5–3.0)
R_{0diff}	The difference between R_{0max}, and R_0 at $q = q_{mid}$.	NA	1.10–1.20 (0.6–1.2)	0.60–1.18 (0.6–1.2)	0.86–1.18 (0.6–1.2)	0.70–1.17 (0.6–1.2)	0.65–1.09 (0.6–1.2)	0.72–1.12 (0.6–1.2)
q_{min} (g/kg)	The absolute humidity value at which $R_0 = R_{0max}$ when $T = T_c$; the minimum value of absolute humidity permitted.	NA	NA	7.7–8.0 (2.0–8.0)	2.2–4.0 (2.0–8.0)	2.0–3.6 (2.0–8.0)	2.1–3.4 (2.0–8.0)	2.1–3.7 (2.0–8.0)
q_{max} (g/kg)	The absolute humidity value at which $R_0 = R_{0max}$ when $T = T_c$; the maximum value of absolute humidity permitted.	NA	NA	22.6–23.0 (16.0–23.0)	17.0–20.0 (16.0–23.0)	17.0–19.0 (16.0–23.0)	18.0–19.0 (16.0–23.0)	17.0–19.0 (16.0–23.0)
q_{mid} (g/kg)	The absolute humidity value at which $R_0 = R_{0max} - R_{0diff}$.	NA	NA	12.6–13.0 (10.0–13.0)	10.2–11.3 (10.0–13.0)	10.2–12.5 (10.0–13.0)	10–12.2 (10.0–13.0)	10.2–12.6 (10.0–13.0)
T_c (˚C) [33,35]	The cutoff temperature above which temperature negatively impacts R_0.	NA	NA	NA	20.24–24.0 (20–25)	20.04–24.46 (20–25)	20.16–24.47 (20–25)	20.52–23.87 (20–25)
T_{diff} (˚C)	A parameter that, when subtracted from T_c, yields the minimum temperature permitted as a model input.	NA	NA	NA	0.40–5.09 (0–15)	1.28–7.05 (0–15)	1.34–5.31 (0–15)	0.77–4.46 (0–15)
T_{exp}	An exponent determining the strength of the impact of temperature on R_0.	NA	NA	NA	0.95–1.54 (0.5–2.0)	0.67–1.49 (0.5–2.0)	0.78–1.33 (0.5–2.0)	0.78–1.34 (0.5–2.0)
D (days) [12,30,31,38]	The duration of influenza infection.	3.35–3.71 (2–5)	4.68–4.98 (2–5)	2.56–4.99 (2–5)	4.05–4.99 (2–5)	3.50–4.70 (2–5)	3.87–4.98 (2–5)	3.67–4.90 (2–5)
L (days) [12,22,23,36,38]	The duration of influenza immunity; in the AH/T/Vary model, the duration of immunity among those who do not lose immunity at an accelerated rate.	369–391 (365–3650)	421–607 (365–3650)	1298–2860 (365–3650)	376–489 (365–3650)	536–838 (365–3650)	310–451 (183–548)	374–567 (365–3650)
L_S (days)	The duration of influenza immunity among those with accelerated immunity loss in the AH/T/Vary model.	NA	NA	NA	NA	NA	NA	82–336 (30–365)
ρ	The proportion of the population with accelerated immunity loss in the AH/T/ Vary model.	NA	NA	NA	NA	NA	NA	0.0006–0.29 (0–0.5)
S_0	The number of people susceptible to influenza at the beginning of the model run.	48.78%-76.16% (40%-80%)	78.77%-79.98% (40%-80%)	71.58%-79.71% (40%-80%)	59.27%-76.79% (40%-80%)	57.03%-69.86% (40%-80%)	67.03%-77.61% (40%-80%)	66.02%-79.36 (40%-80%)
I_0	The number of people infected at the beginning of the model run.	520–1489 (500–1500)	534–851 (500–1500)	611–1161 (500–1500)	515–1052 (500–1500)	512–1105 (500–1500)	515–900 (500–1500)	519–1256 (500–1500)
p [29]	An exponent to allow for imperfect mixing. Homogenous mixing occurs when $p = 1.0$.	0.97	0.97	0.97	0.97	0.97	0.97	0.97

https://doi.org/10.1371/journal.pcbi.1009050.t001

where ρ is the proportion of the model population that loses immunity after a short period L_s and $\beta_{t-L_s} I^p_{t-L_s} S_{t-L_s}$ represents the number of new infections L_s days ago, who would lose their immunity on day t. We note that, since longer-term immunity is lost at an exponential rate, while short term immunity simply removes a set number of individuals from the recovered compartment at each time step, there is a possibility of double-counting. However, given the difference in time scales (less than one year vs. several years), we do not anticipate that this approximation will lead to severe problems.

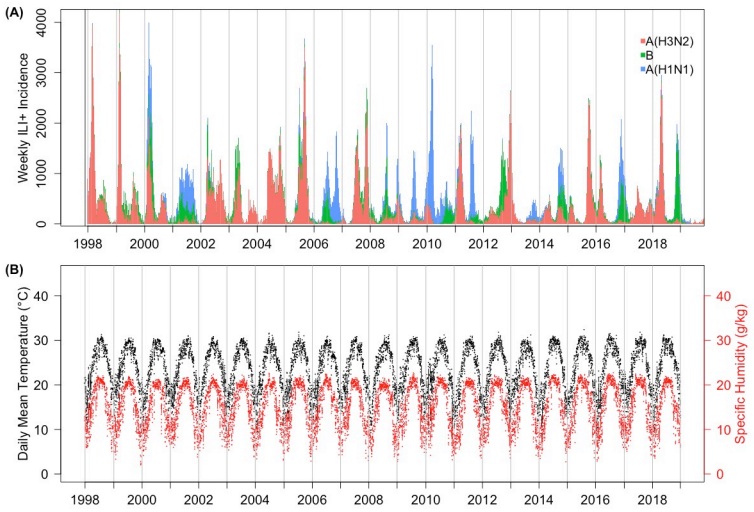

Fig 1. Influenza epidemics observed in Hong Kong during 1998–2018 and the corresponding mean daily temperature and AH. Upper panel: stacked barplot of the weekly ILI+ incidence time series. Segments of the bar represent different virus (sub)types circulating during the week. Lower panel: daily mean temperature and specific humidity (a measure of AH) observed during 1998–2018.

https://doi.org/10.1371/journal.pcbi.1009050.g001

Climate Forcing Models. Based on past work [12,14,16,20], as well as the patterns observed in the influenza and climate data described above and shown in Fig 1, we modeled the impact of AH using a parabola, where transmissibility is highest at very low and very high levels of AH. In all AH/T models, this relationship was modified by temperature such that, when temperature is above some cutoff value, transmissibility is reduced. Specifically, for models AH/T, AH/T/Strain, AH/T/Short, and AH/T/Vary, the impact of AH and temperature on transmissibility was modeled as:

$$R_0(t) = [aq^2(t) + bq(t) + c]\left[\frac{T_c}{T(t)}\right]^{T_{exp}} \quad (3)$$

where $q(t)$ is specific humidity (i.e., a measure of AH) at time t, and $T(t)$ is temperature at time t. The parameter β_t in the SIRS model is defined as $R_0(t)$ divided by D; thus, AH and temperature act through β in Eqs 1 and 2 to influence transmission patterns. When T is below T_c, lower temperatures are able to further increase R_0, whereas temperatures above T_c inhibit influenza transmission. However, the favorable impact of low temperature may level off at relatively low temperatures. Thus, we truncated this monotonic relationship at a minimum temperature of $T_c - T_{diff}$, beyond which, the effect levels off. The strength of this relationship is further determined by the exponent T_{exp}. For the AH Only model, AH was also modeled as a parabola (i.e., the terms within the first set of squared brackets), but with no impact of temperature (Eq S6). In addition, we tested another model combining the temperature response as in Eq 3 and the Null2 model; however, we did not include this model in our main analysis, because conceptually this model is unlikely for (sub)tropical climates (see details in S1 Text).

To link the coefficients a, b, and c to the AH q and R_0, we reparametrize them by solving the parabola with the nadir at (q_{mid}, R_{0min}) and maximum at both (q_{min}, R_{0max}) and (q_{max}, R_{0max}) (see S1 Text).

Model optimization (parameter tuning)

To assess the validity of the models, we first split the influenza data into a training set (Jan 1998 –Dec 2012; 15 years) and a testing set (Jan 2013 –Dec 2018; 6 years). That is, data from 1998 to 2012 were used to train the model and optimize parameters, the remaining data from 2013 to 2018 were held out for testing.

We optimized each model by testing a wide range of parameter values (Table 1) based on the literature [12,22,23,33–39], and tuning parameter range against the influenza data observed during Jan 1998 –Dec 2012 (i.e., the training period). Specifically, for each model, we draw 1 million parameter combinations from ranges listed in Table 1 using Latin hypercube sampling [12]. Using each parameter combination, we ran each model stochastically from Jan 1998 to Dec 2012 with a daily time step and aggregated the simulated daily ILI+ to weekly intervals for model assessment. To account for model stochasticity, we repeated the simulation 500 times for each parameter set. We then calculated, for each model run, the corresponding root mean square error (RMSE) and correlation against the full training dataset and weekly averaged dataset (i.e., for each of the 52 weeks of the year, averaged the ILI+ over 15 training years), separately; We refer to these metrics as *full.RMSE*, *avg.RMSE*, *full.Correlation* and *avg.Correlation*, respectively, hereafter. We further averaged across the 500 model runs for each parameter combination to obtain a single set of metrics for the corresponding parameter combination. To combine the metrics and simplify the process of parameter selection, we averaged the two RMSE metrics (RMSES) and the two correlation metrics (CORR), separately, as:

$$RMSES = 0.5\, full.RMSE + 0.5\, avg.RMSE$$

and:

$$CORR = 0.5\, full.Correlation + 0.5\, avg.Correlation$$

Based on these two final metrics, we selected the top 1000 parameter combinations out of the one million for each model: the 1000 with the highest *CORR* among those with RMSES lower than the 0.5 percentile. We then computed the 95% highest density interval (HDI) for each parameter using those top 1000 to generate new parameter ranges for subsequent round of optimization. That is, we updated the range of a parameter with the HDI, if the upper (or lower) bound of HDI is 10% smaller (or larger) than the corresponding bound of the original range. This tuning process was repeated until the parameter range no longer shrinks substantially (i.e., by 10%). In this study, it took two rounds of such parameter selection; at each round, we checked to ensure the model fit was improving using the new parameter ranges.

After obtaining the final parameter ranges, we drew 10,000 random parameter combinations from these final ranges and ran the models from Jan 1998 –Dec 2018 using each parameter combination. In this last batch, we obtained the top 1000 parameter combinations as described above for further assessment and model comparison.

Model assessment

We evaluated performance of the seven models based on the four metrics described above (i.e., *full.RMSE*, *avg.RMSE*, *full.Correlation*, *avg.Correlation*) during both the training and testing period. To quantify the differences in performance among models, we applied the Kruskal-Wallis test to test if the mean rank of different models were similar for each metric. Since significant differences were found between models, we further performed a pairwise comparison using the Nemenyi test with an adjusted p-value of 0.007 (i.e., 0.05 /7). We summarized the model ranking in Table 2 based on model performances including the pandemic period. In

Table 2. The model performance ranking. For each metric and dataset (i.e., training or testing). the rankings are determined by the model's absolute mean rank differences, compared with the best-ranked model, per the Kruskal-Wallis test. Ties indicate there are no significant differences (i.e., $p \geq 0.007$). The mean value of the corresponding metric is also shown in the parentheses.

	Models	Null1	Null2	AH	AH/T	z	AH/T/ Short	AH/T/ Vary
Train	full.RMSE	6 (772)	4 (675)	7 (804)	1 (611)	5 (720)	1 (604)	1 (611)
	avg.RMSE	6 (422)	5 (349)	7 (541)	1 (243)	4 (310)	1 (240)	1 (249)
	full.Correlation	7 (0.12)	5 (0.43)	6 (0.32)	2 (0.53)	4 (0.50)	1 (0.55)	2 (0.52)
	avg.Correlation	7 (-0.16)	5 (0.73)	6 (0.62)	1 (0.87)	1 (0.88)	1 (0.89)	1 (0.87)
	Average rank	6.5	4.75	6.5	1.25	3.5	1	1.25
Test	full.RMSE	6 (620)	2 (478)	5 (613)	2 (479)	7 (676)	2 (492)	1 (470)
	avg.RMSE	6 (434)	2 (237)	5 (422)	2 (249)	6 (476)	4 (274)	1 (228)
	full.Correlation	7 (-0.0005)	5 (0.49)	6 (0.10)	1 (0.54)	1 (0.55)	1 (0.54)	4 (0.52)
	avg.Correlation	7 (-0.0007)	5 (0.76)	6 (0.11)	1 (0.78)	1 (0.78)	1 (0.79)	4 (0.78)
	Average rank	6.5	3.5	5.5	1.5	3.75	2	2.5

https://doi.org/10.1371/journal.pcbi.1009050.t002

addition, as a sensitivity analysis, we ranked the models based on their performances excluding the 2009 pandemic in S1 Table.

Results

General influenza transmission dynamics in Hong Kong

Influenza activity is highly diverse in Hong Kong. Unlike the common wintertime epidemics in temperate regions, during our study period (Jan 1998– Dec 2018), Hong Kong experienced two epidemics per year in most years (17 out of 21; the four exceptions were: Year 2001, 2011, 2012 and 2018; Fig 1A). For years with two epidemics, one epidemic typically occurred during the winter, and the other, usually smaller in magnitude, occurred during the summer (Fig 1A). Usually, there was a single influenza (sub)type predominating during each epidemic, although co-circulation of multiple strains with comparable magnitudes could occur (Fig 1A). While any (sub)type can dominate winter epidemics, summer epidemics were almost always caused by A(H3N2) (15 out of 17 years with summer epidemics; Fig 1A).

Climate conditions in Hong Kong overall and during influenza epidemics

Both mean daily temperature and AH in Hong Kong displayed strong seasonality, where temperature and AH were highest in summer and lowest in winter (Fig 1B). In the hottest days, the mean temperature in Hong Kong can exceed 30˚C (around six days per year), but most of the time, mean temperature was between 15˚C to 30˚C. Hong Kong was also very humid. Compared to the relatively drier and cooler climates in temperate regions, the humid climate in Hong Kong may provide favorable conditions for influenza transmission during the summer despite the high temperatures. In addition, temperature and AH were highly correlated (Pearson's $\rho = 0.94$, $p < 0.001$). Such a high correlation could confound the potential effect on influenza activity due to either climate variable and suggests that simple linear models will not be able to separate such effects.

Models incorporating the impact of humidity and temperature best replicate the influenza dynamic in Hong Kong

In this work, we designed seven models and performed two rounds of parameter selection to obtain the optimized HDI for each parameter in every model, and eventually compared the models using the selected parameter combinations. Among the seven models constructed, the

Null1 model served as a "control" model since it had a constant R_0 that is independent of any climate factors. In other words, if a model failed to outperform the Null1 model, then the proposed relationship between climate factors and the influenza transmission dynamics would not be supported. In addition, we note, again, that we included the 2009 influenza pandemic in our main analysis, because the off-season occurrence of pandemic influenza provided a unique opportunity to test the climate forcing models under more extreme climate conditions. Table 2 shows the model ranking including the pandemic and S1 Table excluding the pandemic. Results are consistent across the two analyses.

Overall, all models incorporating seasonality outperformed the Null1 model, for which R_0 is set to a constant (mean testing rank: 6.5 out of seven models; Table 2 and Fig 2), suggesting the seasonal variation of influenza activity. In addition, while the AH model (i.e., without including temperature as a variable) outperformed the Null1 model, it was consistently inferior when compared to other models (mean testing rank: 5.5 out of 7 models; Table 2, Fig 2). The model failed to capture much of the dynamics observed in Hong Kong, especially in colder months (S2C Fig). This suggests that, in addition to AH, temperate can modulate influenza transmission in Hong Kong.

To test if the monotonic increase in transmission with decreasing AH as observed in temperate regions also applies to the subtropics, we also tested the model by Shaman et al. (i.e., the Null2 model here). The Null2 model was able to better recreate the observed transmission dynamics in Hong Kong than the Null1 and AH model. However, its performance during the training period ranked lower than models additionally incorporating increasing transmission under high AH conditions (i.e., a bimodal relation) (Table 2).

Models incorporating the impact of both AH and temperature improved the model performance significantly (Fig 2). The AH/T models (AH/T, AH/T/Short, AH/T/Vary, and AH/T/Strain) had the best performance among all. Among these four models, the AH/T and AH/T/Short models assumed the same model construct but with different initial ranges for the immunity duration (L). After rounds of parameter selection, the HDI of L eventually converged for the two models (Table 1), as did other parameters. Therefore, we considered these two models to be the same. Indeed, either model ranked among the top two during the

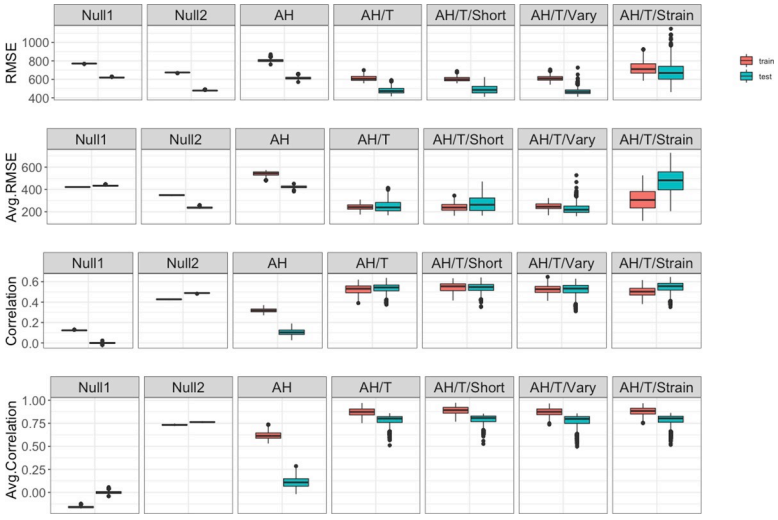

Fig 2. Model performance. Boxes and whiskers show the median (thick horizontal lines), interquartile range and 95% CI of RMSE (1st row), average RMSE (2nd row), correlation (3rd row) and average correlation (4th row) of the top 1000 parameter combinations for each model, during the training (red) and testing (green) period, separately.

https://doi.org/10.1371/journal.pcbi.1009050.g002

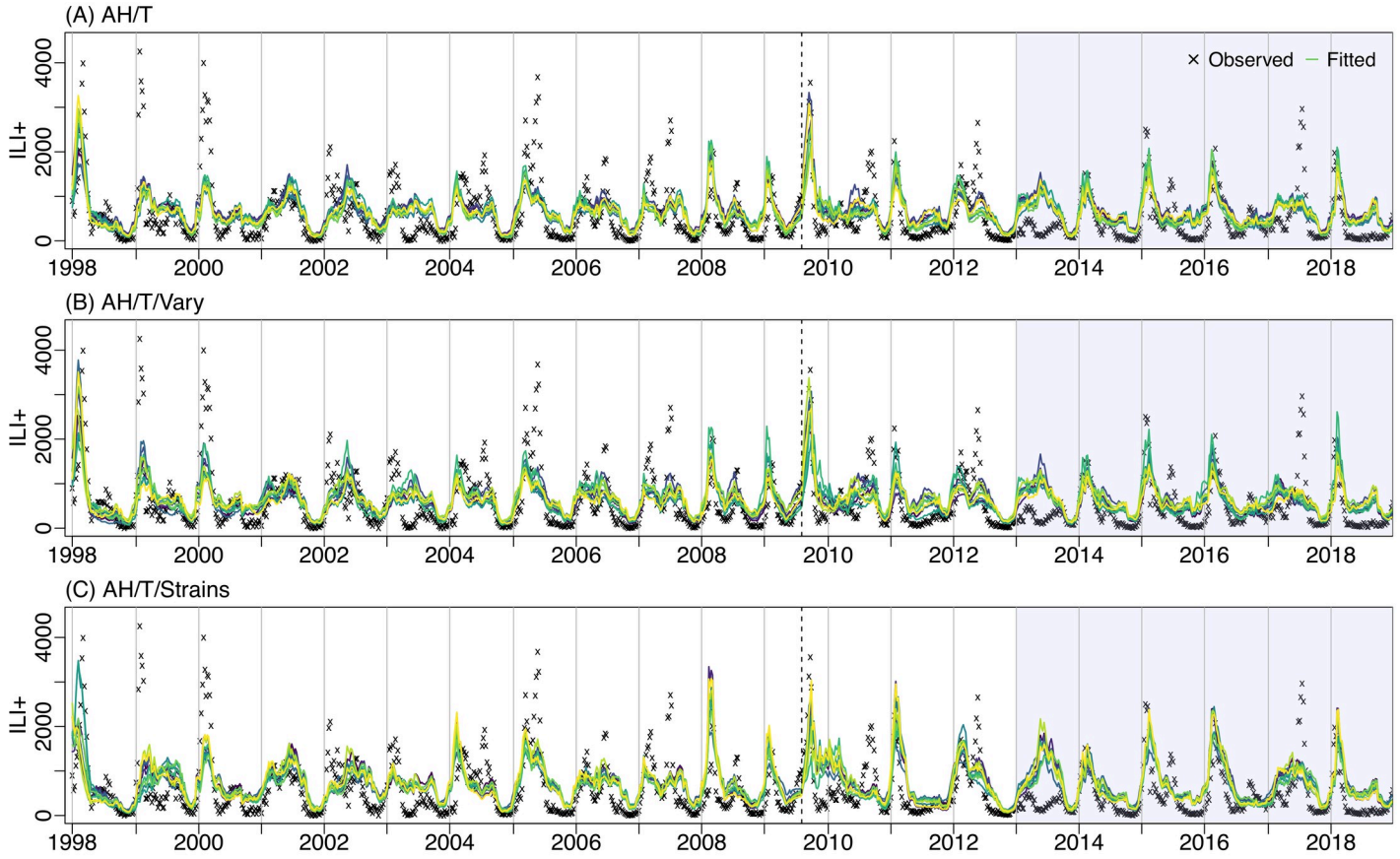

Fig 3. Top 10 model fits for three climate forcing models: AH/T (A), AH/T/Vary (B), and AH/T/Strain (C). Black crosses show observed ILI+; the colored lines run through the crosses are the top 10 model estimates. The vertical dash line indicates a pandemic (2009). The shaded region represents testing years (2013–2018), while the rest are the training years.

https://doi.org/10.1371/journal.pcbi.1009050.g003

training period. However, the AH/T model appeared to be more stable and remained as a top performing model during the testing period (Table 2).

Two models (i.e., AH/T/Vary and AH/T/Strain) additionally accounted for long/short-term immunity and/or co-circulation of different influenza viruses. Both models performed comparably to the AH/T model but not better (Fig 3). In addition, for the common parameters, the HDIs of the three models converged to similar ranges (Table 1). The AH/T/Vary model, although formulated differently, had similar HDI and performances as the AH/T model. The AH/T/Strain model was the only model that specifically accounted for co-circulation of different influenza viruses. Although the model was able to simulate ILI+ with high correlation with the observed data and recreate large epidemics, it did not fit smaller epidemics as well and thus had a high RMSE (Fig 3).

Taken together, the AH/T model had the most consistent and best performance over the entire study period. It is also the most parsimonious model among all top performing ones.

Impact of humidity and temperature on influenza transmission, as estimated by the top models

To account for the impact of humidity on influenza transmission, we included three parameters in the models to describe a bimodal relationship. That is, below a threshold AH (q_{mid}),

transmission would increase as AH decreases and level off when AH is $\leq q_{min}$, whereas above that threshold, transmission would increase as AH increases and level off when AH is $\geq q_{max}$. Tamerius et al 2013 [14] defined a similar bimodal relationship and found a threshold of 11–12 g/kg for regions with single-peak vs bimodal epidemics. In addition, they found that most influenza peak activities occurred in "cold-dry" conditions (i.e., AH < 8 g/kg) or "humid-rainy" conditions (AH > 14 g/kg). Consistent with Tamerius et al., we estimated the threshold q_{mid} to be 10–12.6 g/kg, where R_0 troughs (Fig 4). In addition, we further quantified how influenza transmission (i.e., as indicated by R_0 estimates) changes with AH in the two regimes (Eq 3). We estimated that when AH is below 10–12.6 g/kg, R_0 would increase with decreasing AH quadratically up to a minimum of 2–4 g/kg; when AH is above 10–12.6 g/kg, R_0 would increase with increasing AH quadratically up to a maximum of 17–20 g/kg (Table 1).

In addition to AH, we included three parameters to model the impact of temperature on influenza transmission. Foremost, as described in Eq 3, the impact of temperature is modeled as a multiplicative adjustment to the impact of AH. Below a threshold temperature T_c, decreasing temperature increases transmission up to a minimum of $T_c - T_{diff}$; above T_c, increasing temperature reduces transmission. Deyle et al. [20] suggested temperature around 24˚C (75˚F) as a threshold dividing the negative and positive effect of AH on transmission. Similarly, we estimated T_c to have an HDI between 20–24˚C (Table 1). As shown in Fig 4, when temperature is below T_c, low temperature further facilitates transmission, in addition to the favorable transmission conditions due to concurrent, low AH in cold months. However, when temperature exceeds T_c, high temperature suppresses transmission and lowers the overall R_0 despite the favorable transmission conditions due to concurrent, very high AH in the summer. In addition, we estimated T_{diff} to have an HDI of 0.4–5.3˚C, which implies temperature below 16–23˚C does not afford additional increases in transmission. Similar transmission behavior was also found by Brown et al. [33] with avian influenza viruses, whose infectiveness stabilized after the temperature dropped below 17˚C. The estimated value of T_{exp}, the exponent of the T_c/T ratio (Eq 3), had an HDI of 0.95–1.54, suggesting the moderation of temperature is slightly super-linear.

We also estimated the duration of immunity (L) with our models to better understand transmission dynamics. The immunity period L directly affects the frequency of influenza epidemics–i.e., shorter L would lead to more frequent epidemics. Here we estimated L to be

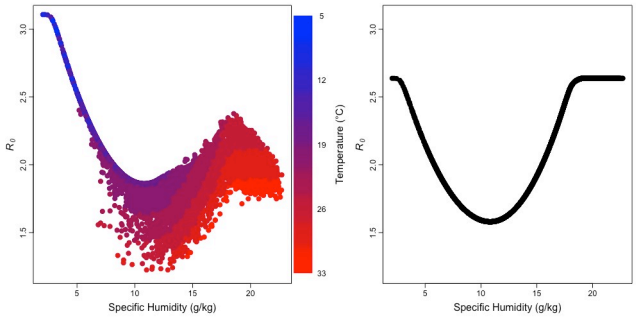

Fig 4. Estimated relationship between influenza transmission with AH and temperature. We use the basic reproductive number (R_0) to represent the level of influenza transmission. Each point shows the estimated R_0 at different specific humidity, a measure of AH, (and temperature if included) calculated per the AH/T model (left) or the AH model (right) using the top 10 parameter combinations for the corresponding model. For the AH/T model (left panel), the color of the point shows the concurrent temperature included in the model to moderate the relationship between R_0 and specific humidity.

https://doi.org/10.1371/journal.pcbi.1009050.g004

around 1–1.3 years for the AH/T model, and 1.5–2.3 year for AH/T/Strain. For the AH/T/Vary model, considering population heterogeneity, we included another parameter L_s to represent short-term immunity (<1 year). We found L_s was around 3–11 months and L around 1–1.6 years; combing these two parameters (i.e., L, Ls), the average is very similar to the L estimated by the AH/T model. Overall, these L estimates are consistent with the frequent influenza epidemics observed in Hong Kong; however, we note that these estimates are on the lower end of the reported 1–10 year range [22].

Validate model findings using laboratory results

The reproductive number represents the epidemic potential of an infection. To examine if the identified relationship with AH and temperature is consistent with data from laboratory studies, we further compared the basic reproductive number R_0 and effective reproductive number R_e calculated by our AH/T model (Eq 3) with the influenza virus survival rate in aerosols [35] as well as the influenza transmission rate observed in guinea pigs [39,40]. At the population level, an epidemic can occur when R_e is above 1 and will subside when R_e drops below 1. Indeed, no transmission occurred in the guinea pig studies [40] under conditions where the estimated R_e per our model (Eq 3) was below 1; in contrast, transmission occurred when estimated R_e was above 1, ranging 1.21–2.25 (corresponding R_0 range: 1.68–3.11; Fig 5). In addition, fitting a linear regression model of estimated R_0 (or R_e) against the log survival rate and log transmission probability, we found that estimated R_0 (or R_e) positively correlated with both laboratory-observed survival rate and transmission rate of the influenza virus (Fig 5). In particular, the correlation between R_0 (or R_e) estimated by our AH and temperature model (Eq 3) and the observed transmission rate was 0.82 ($r^2 = 0.67$; Fig 5), suggesting it was able to explain around 70% of the variances of the transmission rate. In comparison, overall, the Null2 and AH models did not perform as well (S4 and S5 Figs). These findings indicate that our model is able to represent both the impact of AH and temperature on influenza epidemic patterns at the population level as well as influenza transmission and survival observed in laboratory settings.

Discussion

Despite influenza's profound impact on public health, little is known about how the virus transmits from person to person and what environmental and climate conditions make this process more likely. To date, there have been only a few studies on the influenza burden in tropical and subtropical regions. Of those studies, a handful analyzed the effect of climate drivers on influenza incidence using time-series or logistic regression models. Although those statistical models were able to identify significant climate covariates (including AH, temperature, and precipitation) and estimate the effect size, they did not provide much information to the underlying mechanism of how those climate covariates affect transmission. In contrast, infectious disease models (e.g., the SIRS model) provide a means to model and test the relationship between climate factors and influenza transmission observed in laboratories. In this work, by building seven SIRS models under different hypotheses, we explored how temperature, AH, and influenza co-circulation affect the transmission of influenza. We showed that models that included both AH and temperature as covariates consistently outperformed those that did not in recreating the observed influenza epidemic patterns in Hong Kong. These results support that climate variables play a critical role in influenza transmission, where temperature is particularly influential in moderating the impact of AH. Model results also indicate that the effect of climate drivers in tropical and sub-tropical regions is different from those observed in the temperate regions, and models built for temperate areas will not be sufficient to reproduce the transmission patterns in the tropics or the subtropics.

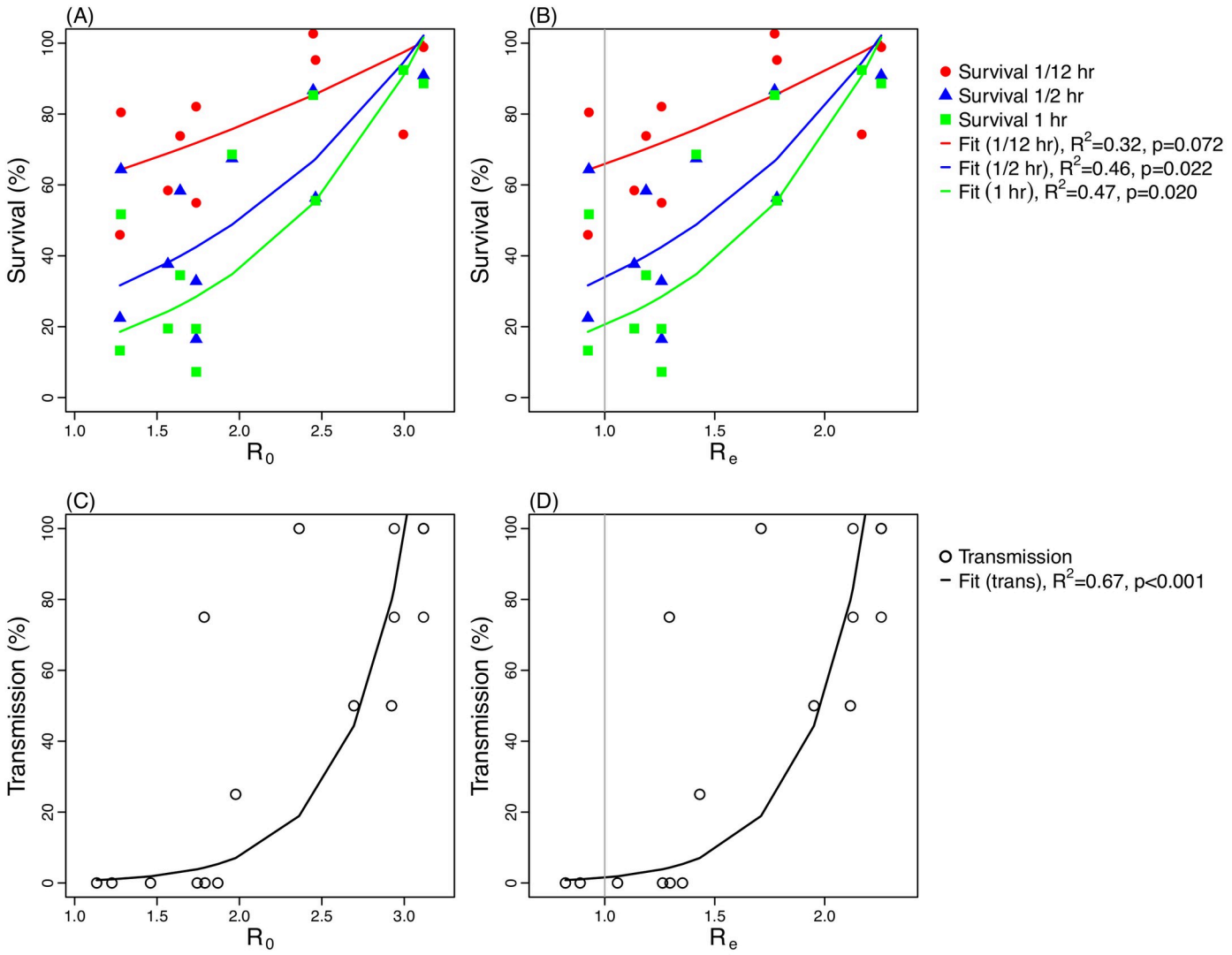

Fig 5. Comparison of the reproductive numbers estimated by the AH/T model with laboratory observed virus survival rate and transmission rate in guinea pigs. Left panel plots the viral survival rate (A) and transmission rate (C) against R_0 calculated using Eq 3 and best-fit parameters for the AH/T model. Right panel plots the viral survival rate (B) and transmission rate (D) against R_e, where R_e is calculated as R_0 multiplied by the estimated mean population susceptibility during the study period. The grey vertical line indicates where R_e = 1. The viral survival data came from Harper 1961 [35] and transmission rate data came from Lowen et al. 2007 and 2008 [39,40].

https://doi.org/10.1371/journal.pcbi.1009050.g005

Previous studies had suggested a bimodal effect of AH on influenza transmission [20]. However, such an effect has not been quantified nor incorporated in influenza transmission models as done for temperate regions [12]. Here, we have developed a model that can effectively represent this U-shaped relationship with AH, moderated further by temperature. When incorporated into an SIRS model, the combined model was able to recreate the diverse influenza epidemic dynamics observed in Hong Kong over a 21-year period. As described earlier, the breaking point between the "cold-dry" and "hot-humid" environment is an AH of approximately 10–12.6 g/kg, which is consistent with Tamerius et al 2013 [14]. This finding helps to explain the biannual epidemics observed in Hong Kong. In the winter when weather is "cold-dry," the influenza transmission rate increases as the environment gets drier. On the other

hand, summer in Hong Kong is hot and humid–the very high AH also promotes influenza transmission, despite high temperatures.

The combined relationship of influenza transmission with both AH and temperature we delineated in Fig 4 also consistently explains observations in temperate regions where influenza surges predominantly in winter and increases monotonically with decreasing AH. During summers in temperate areas, absolute AH is typically lower than 15 g/kg (vs. as high as 23g/kg in subtropics/tropics) [12], and temperature is relatively high. Under such environmental conditions, R_0 would stay in the trough during the summer (Fig 4), and only increases in the winter when AH becomes low (Fig 4). As such, it appears that influenza transmission rate increases monotonically with decreasing AH, leading to a single epidemic each year in the winter in temperate regions.

In addition, the seasonality–i.e., the relationship of influenza transmission with AH and temperature–identified here also appears to be robust for both seasonal epidemics and the 2009 pandemic. After accounting for the higher susceptibility to the novel 2009 A(H1N1) influenza virus, our best-performing models were able to capture the trends during the pandemic using the same climate forcing functions as for seasonal epidemics. This finding further supports a causal mechanism underlying this seasonality. However, we note that disease seasonality does not imply a disease can only occur during a certain time of the year. Rather, in addition to the seasonality, the exact timing of influenza epidemics is also the result of population susceptibility, contact patterns, and emergence of new influenza viruses (e.g., antigenic innovations) and their introduction to local populations. In particular, the population susceptibility to influenza and the global circulation of influenza viruses have changed during the COVID-19 pandemic due to the implemented non-pharmaceutical interventions and behavioral changes [41]. This may in turn alter the timing of influenza epidemics after the COVID-19 pandemic (likely temporally) [42], despite the same seasonality. Thus, models should take these population and viral changes into account when modeling and forecasting future influenza epidemics.

When there are multiple strains co-circulating, individuals who recover from infection gain specific immunity against the infecting strain and may remain susceptible to other influenza strains in co-circulation either during the same or subsequent epidemics. In this study, we combined data from all three co-circulating influenza viruses and, as such, our estimated duration of immunity, without distinguishing specific strains, was relatively short (~1–1.5 years). In comparison, the AH/T/Strain model which modeled H3N2 and H1N1/B epidemics separately, estimated a longer immunity period (1.5–2.5 years). Nevertheless, either estimate is quite low compared to the duration an influenza clade in circulation (1–10 years). Therefore, we note that the short immunity duration estimated here is more to capture the frequent influenza epidemics in Hong Kong. For locations with less frequent influenza epidemics, re-estimating the immunity duration per local epidemic data is warranted.

We recognize several limitations of our study. First, although our models fit the observations in Hong Kong well and provide support to the role of AH and temperature on influenza transmission, it is important to note that further laboratory and epidemiologic works are needed to establish a causal relationship. Second, while we accounted for multi-strain co-circulation to some extent (e.g., the AH/T/Short and the AH/T/Strain model), our models are highly simplified and do not distinguish the different epidemiological characteristics for H3N2, H1N1, and B; as such, our estimate of the immunity period may not reflect the true value. Third, for model simplicity, we did not model the interactions between (sub)types, which can modify the association with climate variables [43]. Future research is necessary to explore the impact of co-circulation, as a reasonable inclusion of multiple influenza (sub)types may be more appropriate than combining all strains. Fourth, as a first step, here we combined

all influenza viruses without separating influenza by subtype or type. Previous studies have reported differential responses of different influenza strains to climate variables [43]. Future work could also model the impact of climate variables for each influenza virus separately to examine such potential differences and the impact on influenza epidemic dynamics at the population level.

Our study also sidestepped several key factors that may shape influenza transmission dynamics, in particular, age, vaccination, and seasonal changes in contact patterns. Due to a lack of age-specific incidence data, we did not include age structure in our models. Vaccination rate in Hong Kong has increased in recent years, particularly among children aged <12 years and adults 65 years or older, due to vaccination subsidy provided to these age groups from 2008 onwards [44–46]. For instance, vaccination rate among children aged <12 years increased from 9.7% in 2011/12 to 55.4% in 2018/19; and vaccination rate among adults 65+ increased from 31.7% in 2011/12 to 43.6% in 2018/19 [47,48]. These increases in vaccination coverage may in part explain the apparent decreases in ILI+ in recent years; a one-sided *t*-test indicated that the yearly ILI+ during 2011–2018 were significantly lower than years before 2009 (i.e., excluding the 2009 pandemic period; $p = 0.009$). However, we do not have detailed data on vaccination rate nor vaccine efficacy over the entire study period in order to account for the impact of vaccination. Further, seasonal changes in contact patterns could also contribute to the observed seasonal influenza epidemic dynamics in Hong Kong. For instance, during a hot, humid summer, people may spend more time indoors and thus create additional opportunities for onward transmission to occur. Similar increases of indoor contact and transmission could occur during colder days in the winter. As such, the increased transmission under highly humid conditions in the summer or colder-drier conditions in the winter may be in part due to increased contact indoors, in addition to the higher survival rate of influenza viruses under these environmental conditions as shown in laboratory studies [15,16,39]. Our modeling here is not able to tease this apart. Future work is warranted to incorporate these additional factors that may further improve understanding of influenza transmission dynamics in tropical and subtropical climates. Nevertheless, we note that, all climate forcing models tested here are subject to the same limitations discussed above. Thus, the relative performance of the models and our general findings regarding key climate drivers still hold.

In summary, we have developed a simple mechanistic model incorporating the impact of AH and temperature on influenza transmission that is able to recreate the long-term influenza epidemic dynamics in Hong Kong, a subtropical city with highly diverse epidemic patterns. Past work has demonstrated that, incorporating information on AH into mechanistic influenza models significantly improved model fit and forecast accuracy in temperate regions [11]. Given that forecasts in the tropics and subtropics tend to be substantially less accurate than forecasts in temperate regions [36], the climate forcing model developed here could support a better understanding of climatic drivers of influenza transmission in these regions. Future work could incorporate this model into an SIRS model-forecast system to improve forecast accuracy in the tropics and subtropics to aid public health and medical workers in better anticipating influenza transmission in forthcoming weeks.

Supporting information

S1 Fig. The change of mean ILI+ of each influenza (sub)type in circulation within a year. The mean ILI+ took average of the ILI+ observed in Hong Kong over 21 years (1998–2018). (TIF)

S2 Fig. Top 10 model fits for Null1 (A), Null2 (B), and AH (C) model. Black crosses show observed ILI+; the colored lines run through the crosses show the top 10 model estimates. The

vertical dash line indicates the onset of the 2009 pandemic. The shaded regions indicate testing years (2013–2018); and the rest are the training years.
(TIF)

S3 Fig. Top 10 model fits for the observed seasonality (averaged over training or testing years) for the seven models: Null1 (A), Null2 (B), AH (C), AH/T (D), AH/T/Short(E) AH/T/Vary (F) and AH/T/Strain (G). Black crosses show observed averaged ILI+ over training or testing years; colored lines run through the crosses show the top 10 model estimates. Left panels show model fits for the training period and the right panels show model fits for the testing period.
(TIF)

S4 Fig. Comparison of the reproductive numbers estimated by the *Null2* model with laboratory observed virus survival rate and transmission rate in guinea pigs. Same as in Fig 5 but using the Null 2 model instead.
(TIF)

S5 Fig. Comparison of the reproductive numbers estimated by the *AH* model with laboratory observed virus survival rate and transmission rate in guinea pigs. Same as in Fig 5 but using the AH model instead.
(TIF)

S6 Fig. Sensitivity analysis on the seeding parameter α: model fits and estimates for other model parameters and variables. To test the model sensitivity to the value of α, we ran the AH/T model along with the SIRS model using five different values (ranging from 1/30 to 1 as specified in the legend), separately. We optimized the model for each setting per the same procedure as described in the main text to estimate other parameters and variables.
(TIF)

S1 Table. The model performance ranking, *excluding the 2009 pandemic*. For each metric and dataset (i.e., training or testing). the rankings are determined by the model's absolute mean rank differences, compared with the best-ranked model, per the Kruskal-Wallis test. Ties indicate there are no significant differences (i.e., $p \geq 0.007$). The mean value of the corresponding metric is also shown in the parentheses.
(XLSX)

S2 Table. The model performance ranking, *including the Null2/T model*. For each metric and dataset (i.e., training or testing). the rankings are determined by the model's absolute mean rank differences, compared with the best-ranked model, per the Kruskal-Wallis test. Ties indicate there are no significant differences (i.e., $p \geq 0.006$). The mean value of the corresponding metric is also shown in the parentheses.
(XLSX)

S1 Text Supplementary document includes 1) Preliminary data processing; 2) Simulation methods and Modeling detail; 3) Additional modeling results.
(DOCX)

Acknowledgments

We thank the Hong Kong Center for Health Protection for providing data on sentinel surveillance and laboratory surveillance for influenza. We also thank Columbia University Mailman School of Public Health for access to high performance computing.

Author Contributions

Conceptualization: Benjamin J. Cowling, Wan Yang.

Data curation: Eric H. Y. Lau, Benjamin J. Cowling.

Formal analysis: Haokun Yuan, Sarah C. Kramer, Wan Yang.

Funding acquisition: Benjamin J. Cowling, Wan Yang.

Investigation: Haokun Yuan, Sarah C. Kramer, Eric H. Y. Lau, Benjamin J. Cowling, Wan Yang.

Methodology: Haokun Yuan, Sarah C. Kramer, Wan Yang.

Supervision: Wan Yang.

Validation: Haokun Yuan, Sarah C. Kramer.

Visualization: Haokun Yuan, Sarah C. Kramer.

Writing – original draft: Haokun Yuan, Sarah C. Kramer, Wan Yang.

Writing – review & editing: Haokun Yuan, Sarah C. Kramer, Eric H. Y. Lau, Benjamin J. Cowling, Wan Yang.

References

1. World Health Organization. *Influenza (Seasonal) 2018* [Available from: https://www.who.int/en/news-room/fact-sheets/detail/influenza-(seasonal).
2. Wong CM, Yang L, Chan KP, Leung GM, Chan KH, Guan Y, et al. Influenza-Associated Hospitalization in a Subtropical City. PLoS Medicine. 2006; 3(4):e121–e. https://doi.org/10.1371/journal.pmed.0030121 PMID: 16515368
3. Ng S, Gordon A. Influenza Burden and Transmission in the Tropics. Current Epidemiology Reports. 2015; 2(2):89–100. https://doi.org/10.1007/s40471-015-0038-4 PMID: 25938010
4. Chretien J-P, George D, Shaman J, Chitale RA, McKenzie FE. Influenza Forecasting in Human Populations: A Scoping Review. PLoS ONE. 2014; 9(4):e94130–e. https://doi.org/10.1371/journal.pone.0094130 PMID: 24714027
5. Nsoesie EO, Brownstein JS, Ramakrishnan N, Marathe MV. A systematic review of studies on forecasting the dynamics of influenza outbreaks. Blackwell Publishing; 2014. p. 309–16.
6. Cummings MJ, Bakamutumaho B, Kayiwa J, Byaruhanga T, Owor N, Namagambo B, et al. Epidemiologic and spatiotemporal Characterization of influenza and severe acute respiratory infection in Uganda, 2010–2015. Annals of the American Thoracic Society. 2016; 13(12):2159–68. https://doi.org/10.1513/AnnalsATS.201607-561OC PMID: 27612095
7. Soebiyanto RP, Clara W, Jara J, Castillo L, Sorto OR, Marinero S, et al. The Role of Temperature and Humidity on Seasonal Influenza in Tropical Areas: Guatemala, El Salvador and Panama, 2008–2013. PLoS ONE. 2014; 9(6):e100659–e. https://doi.org/10.1371/journal.pone.0100659 PMID: 24956184
8. Yang L, Ma S, Chen PY, He JF, Chan KP, Chow A, et al. Influenza associated mortality in the subtropics and tropics: Results from three Asian cities. Vaccine. 2011; 29(48):8909–14. https://doi.org/10.1016/j.vaccine.2011.09.071 PMID: 21959328
9. Tamerius J, Nelson MI, Zhou SZ, Viboud C, Miller MA, Alonso WJ. Global influenza seasonality: Reconciling patterns across temperate and tropical regions. Environmental Health Perspectives. 2011; 119(4):439–45. https://doi.org/10.1289/ehp.1002383 PMID: 21097384
10. Bloom-Feshbach K, Alonso WJ, Charu V, Tamerius J, Simonsen L, Miller MA, et al. Latitudinal Variations in Seasonal Activity of Influenza and Respiratory Syncytial Virus (RSV): A Global Comparative Review. PLoS ONE. 2013; 8(2):e54445–e. https://doi.org/10.1371/journal.pone.0054445 PMID: 23457451
11. Shaman J, Kohn M. Absolute humidity modulates influenza survival, transmission, and seasonality. Proceedings of the National Academy of Sciences of the United States of America. 2009; 106(9):3243–8. https://doi.org/10.1073/pnas.0806852106 PMID: 19204283

12. Shaman J, Pitzer VE, Viboud C, Grenfell BT, Lipsitch M. Absolute humidity and the seasonal onset of influenza in the continental United States. PLoS Biology. 2010; 8(2). https://doi.org/10.1371/journal.pbio.1000316 PMID: 20186267

13. Shek LP-C, Lee B-W. Epidemiology and seasonality of respiratory tract virus infections in the tropics. Paediatric Respiratory Reviews. 2003; 4(2):105–11. https://doi.org/10.1016/s1526-0542(03)00024-1 PMID: 12758047

14. Tamerius JD, Shaman J, Alonso WJ, Bloom-Feshbach K, Uejio CK, Comrie A, et al. Environmental Predictors of Seasonal Influenza Epidemics across Temperate and Tropical Climates. PLoS Pathogens. 2013; 9(3). https://doi.org/10.1371/journal.ppat.1003194 PMID: 23505366

15. Lowen AC, Steel J. Roles of Humidity and Temperature in Shaping Influenza Seasonality. Journal of Virology. 2014; 88(14):7692–5. https://doi.org/10.1128/JVI.03544-13 PMID: 24789791

16. Yang W, Elankumaran S, Marr LC. Relationship between Humidity and Influenza A Viability in Droplets and Implications for Influenza's Seasonality. PLoS ONE. 2012; 7(10):1–8.

17. Moura FEA, Furtado RM, Teófilo R, Perdigão ACB, Siqueira MM. Seasonality of Influenza in the Tropics: A Distinct Pattern in Northeastern Brazil. 2009.

18. Lutwama JJ, Bakamutumaho B, Kayiwa JT, Chiiza R, Namagambo B, Katz MA, et al. Clinic-and hospital-based sentinel influenza surveillance, Uganda 2007–2010. Journal of Infectious Diseases. 2012; 206(SUPPL.1). https://doi.org/10.1093/infdis/jis578 PMID: 23169978

19. Mahamat A, Dussart P, Bouix A, Carvalho L, Eltges F, Matheus S, et al. Climatic drivers of seasonal influenza epidemics in French Guiana, 2006–2010. Journal of Infection. 2013; 67(2):141–7. https://doi.org/10.1016/j.jinf.2013.03.018 PMID: 23597784

20. Deyle ER, Maher MC, Hernandez RD, Basu S, Sugihara G. Global environmental drivers of influenza. Proceedings of the National Academy of Sciences of the United States of America. 2016; 113 (46):13081–6. https://doi.org/10.1073/pnas.1607747113 PMID: 27799563

21. Carrat F, Flahault A. Influenza vaccine: The challenge of antigenic drift. 2007. p. 6852–62.

22. Liu M, Zhao X, Hua S, Du X, Peng Y, Li X, et al. Antigenic Patterns and Evolution of the Human Influenza A (H1N1) Virus. Scientific Reports. 2015;5. https://doi.org/10.1038/srep14171 PMID: 26412348

23. Smith DJ, Lapedes AS, De Jong JC, Bestebroer TM, Rimmelzwaan GF, Osterhaus ADME, et al. Mapping the antigenic and genetic evolution of influenza virus. Science. 2004; 305(5682):371–6. https://doi.org/10.1126/science.1097211 PMID: 15218094

24. Couch RB, Kasel JA. Immunity to Influenza in Man. Annual Review of Microbiology. 1983; 37(1):529–49. https://doi.org/10.1146/annurev.mi.37.100183.002525 PMID: 6357060

25. Greene SK, Ionides EL, Wilson ML. Patterns of Influenza-associated Mortality among US Elderly by Geographic Region and Virus Subtype, 1968–1998. American Journal of Epidemiology. 2006; 163 (4):316–26. https://doi.org/10.1093/aje/kwj040 PMID: 16394205

26. Climatological Information Services|Hong Kong Observatory(HKO)|Climate [cited 2020. Available from: https://www.hko.gov.hk/en/cis/climat.htm.

27. Wallace J, Hobbs P. Atmospheric Science: An Introductory survey. 2nd Edition ed. York New: Academic Press; 2006. 504 p.

28. Census and Statistics Department HKSAR. Fertility Trend in Hong Kong, 1981 to 2017. Hong Kong Monthly Digest of Statistics. 2018.

29. Finkenstadt BF, Grenfell BT. Time Series Modelling of Childhood Diseases: A Dynamical Systems Approach. 2000.

30. Roper WL, Hamburg MA, King Holmes DK, Deborah Holtzman W, John Iglehart GK, Maki DG, et al. Serum Cross-Reactive Antibody Response to a Novel Influenza A (H1N1) Virus After Vaccination with Seasonal Influenza Vaccine. 2009.

31. Miller E, Hoschler K, Hardelid P, Stanford E, Andrews N, Zambon M. Incidence of 2009 pandemic influenza A H1N1 infection in England: a cross-sectional serological study. The Lancet. 2010; 375 (9720):1100–8. https://doi.org/10.1016/S0140-6736(09)62126-7 PMID: 20096450

32. Yang W, Lau EHY, Cowling BJ. Dynamic interactions of influenza viruses in Hong Kong during 1998–2018. PLoS Comput Biol. 2020; 16(6):e1007989.

33. Brown JD, Goekjian G, Poulson R, Valeika S, Stallknecht DE. Avian influenza virus in water: Infectivity is dependent on pH, salinity and temperature. Veterinary Microbiology. 2009; 136(1–2):20–6. https://doi.org/10.1016/j.vetmic.2008.10.027 PMID: 19081209

34. Chowell G, Miller MA, Ib ANDCV. Seasonal influenza in the United States, France, and Australia: transmission and prospects for control.

35. Harper GJ. Airborne micro-organisms: survival tests with four viruses. Epidemiology and Infection. 1961; 59(4):479–86. https://doi.org/10.1017/s0022172400039176 PMID: 13904777

36. Kramer SC, Shaman J. Development and validation of influenza forecasting for 64 temperate and tropical countries. PLoS Computational Biology. 2019; 15(2):e1006742–e. https://doi.org/10.1371/journal.pcbi.1006742 PMID: 30811396

37. Mills CE, Robins JM, Lipsitch M. Transmissibility of 1918 pandemic influenza. Nature. 2004; 432 (7019):904–6. https://doi.org/10.1038/nature03063 PMID: 15602562

38. Yang W, Cowling BJ, Lau EHY, Shaman J. Forecasting Influenza Epidemics in Hong Kong. PLoS Computational Biology. 2015; 11(7):1–17. https://doi.org/10.1371/journal.pcbi.1004383 PMID: 26226185

39. Lowen AC, Mubareka S, Steel J, Palese P. Influenza Virus Transmission Is Dependent on Relative Humidity and Temperature. PLoS Pathogens. 2007; 3(10):e151–e. https://doi.org/10.1371/journal.ppat.0030151 PMID: 17953482

40. Lowen AC, Steel J, Mubareka S, Palese P. High Temperature (30˚C) Blocks Aerosol but Not Contact Transmission of Influenza Virus. Journal of virology. 2008; 82(11):5650–2. https://doi.org/10.1128/JVI.00325-08 PMID: 18367530

41. Lee J, Neher R, Bedford T. Real-time tracking of influenza A/H3N2 evolution using data from GISAID 2020 [Available from: https://nextstrain.org/flu/seasonal/h3n2/ha/2y.

42. Baker RE, Park SW, Yang W, Vecchi GA, Metcalf CJE, Grenfell BT. The impact of COVID-19 nonpharmaceutical interventions on the future dynamics of endemic infections. Proc Natl Acad Sci U S A. 2020; 117(48):30547–53. https://doi.org/10.1073/pnas.2013182117 PMID: 33168723

43. Yang W, Cummings MJ, Bakamutumaho B, Kayiwa J, Owor N, Namagambo B, et al. Dynamics of influenza in tropical Africa: Temperature, humidity, and co-circulating (sub)types. Influenza and other Respiratory Viruses. 2018; 12(4):446–56. https://doi.org/10.1111/irv.12556 PMID: 29573157

44. Hong Kong's Department of Health. 2008–2009 Annual Report.

45. Hong Kong's Department of Health. Vaccination subsidy schemes launched [press release]. 2009.

46. Hong Kong's Department of Health. Subsidised vaccination for young children and elderly. 2009.

47. Legistrative Council of the Hong Kong Special Administrative Region of the People's Republic of China. Seasonal Influenza Vaccination 2018 [Available from: https://www.legco.gov.hk/research-publications/english/essentials-1718ise06-seasonal-influenza-vaccination.htm.

48. Centre for Health Protection. Statistics on Vaccination Programmes in the Past 3 years 2020 [Available from: https://www.chp.gov.hk/en/features/102226.html.